Experimental Thermal and Fluid Science 34 (2010) 1049–1056

Contents lists available at ScienceDirect

Experimental Thermal and Fluid Science

journal homepage: www.elsevier.com/locate/etfs

Analysis of heat and mass transfer enhancement in porous material subjected to electric fields (effects of particle sizes and layered arrangement)

Chainarong Chaktranond *, Phadungsak Rattanadecho

Department of Mechanical Engineering, Faculty of Engineering, Thammasat University, Rangsit Campus, Pathumthani 12121, Thailand

ARTICLE INFO

Article history:
Received 23 September 2009
Received in revised form 3 February 2010
Accepted 5 February 2010

Keywords:
Electrohydrodynamics
Drying process
Heat and mass transfer

ABSTRACT

This research experimentally investigates the influences of electrical voltage, particle sizes and layer arrangement on the heat and mass transfer in porous packed bed subjected to electrohydrodynamic drying. The packed bed consists of a single and double layers of glass beads, water and air. Sizes of glass beads are 0.125 and 0.38 mm in diameter. Electric fields are applied in the range of 0–15 kV. Average velocity and temperature of hot airflow are controlled at 0.33 m/s and 60 °C, respectively. The results show that the convective heat transfer coefficient and drying rate are enhanced considerably with a Corona wind. In the single-layered case, due to effects of porosity, the packed bed containing small beads has capillary pressure higher than that with big beads, resulting in higher removal rate of water and higher rate of heat transfer. Considering the effect of capillary pressure difference, temperature distribution and removal rate of moisture in the double-layered case appear to be different than those observed in the single-layered case. Moreover, in the double-layered case, the fine-coarse packed bed gives drying rate higher than that given by the coarse–fine packed bed.

1. Introduction

There has been a continuous effort to achieve a better technological performance in drying processes, which provide high quality products and minimize the energy cost. Hot-air drying technique is widely used in agricultural industries for removing the moisture content from products. However, its drying period is long, resulting in large energy consumption. In order to improve the drying rate, many researchers have paid much attention in a development of hot-air drying by cooperating the conventional method with the other methods, e.g., microwave [1–6], infrared [7–10], and electric fields (Electrohydrodynamics, EHD) [11–13]. In order to increase the removal rate of moisture within materials, microwave irradiation penetrates in the bulk of material, and creates a heat source at a certain location. However, microwave drying is known to result in a poor quality product if it is not properly applied [2,3]. To heat the surface region, infrared radiation is transmitted through water at a short wavelength, while it is absorbed on the surface at a long wavelength [8]. This way of drying process is suitable to dry thin layers of material with large surface exposed to radiation. In electrohydrodynamic drying, high-intensity electric field is applied to airflow in order to induce the secondary flow or circulating flow, so-called Corona wind. The net effect of this secondary flow is additional mixing of fluids and destabilization of boundary layer, therefore leading to a substantial increase in mass transfer coefficients [11].

Due to simultaneous heat and mass transfer taking place during drying process, mechanisms of drying in porous materials are complicated, and still have been investigated by many researchers. Schröder et al. [14] measured heat transfer between particles and nitrogen gas flow in packed bed. They reported that increasing gas flow led to higher heat transport coefficient. Alem-Rajabif and Lai [11] experimentally investigated the drying rate of partially wetted glass bead subjected to electric field. In their experiments, a wire electrode and a copper plate were located on the upper and lower of a packed bed, respectively. The results showed that EHD drying was most effective at the surface of the packed bed. In addition, the rate of drying with the positive Corona was generally greater than that with the negative Corona. This result was consistent with the experimental setup by Alem-Rajabif and Lai [11], Lai and Lai [12] who examined the influence of electric field parameters on the drying rate of a packed bed. Their results showed that drying rate depended on the strength of the electric field and the velocity of the cross flow. Without cross flow, the drying rate increased linearly with the applied voltage, while the influence of Corona wind was suppressed by high cross-flow velocity.

To explain the drying mechanisms, Ratanadecho et al. [4] experimentally and numerically studied the microwave drying in unsaturated material with different porosities. They found that packed bed with a small bead size had capillary forces and drying rate higher than that with a big bead size. From the above literatures,

* Corresponding author. Tel.: +66 02 564 3001x3144; fax: +66 02 564 3010.
E-mail address: cchainar@engr.tu.ac.th (C. Chaktranond).

0894-1777/$ - see front matter © 2010 Elsevier Inc. All rights reserved.
doi:10.1016/j.expthermflusci.2010.02.015

Nomenclature

C	coarse bead
d	diameter of glass bead (mm)
D_h	hydraulic diameter (m)
F	fine bead
h_c	convective heat transfer coefficient (W/m^2 K)
h_v	latent heat of vaporization (J/kg)
K	permeability (m^2)
M	mass (kg)
$\dot{m}$	mass flux of evaporation (kg/m^2 s)
p	pressure (Pa)
R_e	Reynolds number
S	saturation
S_{eff}	effective water saturation associated with the irreducible water saturation
T	temperature (°C)
∇T	temperature gradient in packed bed (°C)
V	volume (m^3)
X	moisture content
z	distance from surface of packed bed

Greek letters

δ	depth of packed bed (mm)
λ_{eff}	the effective thermal conductivity (W/m K)
μ	viscosity (Pa s)
ϕ	porosity (m^3/m^3)
ρ	density (kg/m^3)
σ	surface tension (Pa m)

Subscripts

a	air
c	capillary
eff	effective
EHD	air with electric fields
$free$	free air
g	gas
l	liquid
s	solid
sur	surface
w	water

only the researches by Ratanadecho et al. [4–6] had studied the mechanisms of heat and mass transfer in the packed bed. However, behaviour of microwave heating is different from hot-air heating. To get further understanding in the mechanisms of drying with surface heating, this study experimentally investigates and analyzes the heat and mass transfer within single- and double-layered porous packed bed subjected to hot-air flow and electric fields. Moreover, effects of particle sizes and layered arrangement are also examined.

2. Theory

2.1. Drying enhancement with Corona wind

For drying with hot-air flow, the idea of heat-and-mass transfer enhancement by utilizing EHD is shown in Fig. 1. When hot-air flow exposes to high-voltage electric fields, the flow is circulated. Then this secondary flow enhances the convective heat transfer and depresses the influence of boundary layer on the packed-bed surface. This causes much of moisture on surface to vaporize towards the hot-air flow, and allows larger amount of heat to transfer into the packed bed. Consequently, the drying rate is substantially enhanced.

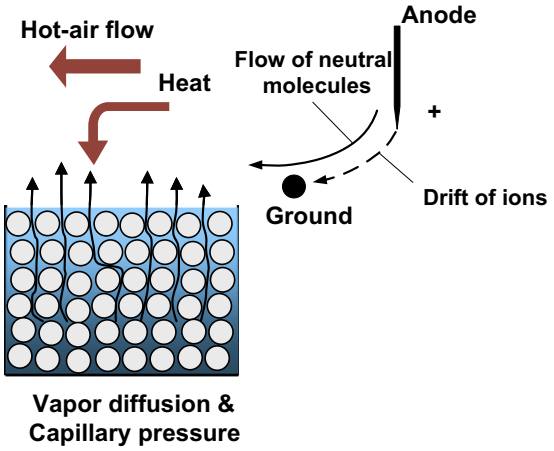

Fig. 1. Idea of enhancement of heat and mass transfer with corona wind.

2.2. Related equations

Water saturation (S) of a porous medium with respect to a particular fluid is defined as

$$S = \frac{\text{Volume of fluid}}{\text{Total volume of voids}} = \frac{V_{\text{water}}}{V_{\text{void}}} \tag{1}$$

Moisture content (X) in porous material is the ratio of total mass of water (M_w) to total mass of dry solid (M_s), i.e.

$$X = \frac{M_w}{M_s} \tag{2}$$

Eq. (2) can be written in term of water saturation as,

$$X = \frac{\phi \rho_w}{(1-\phi)\rho_s} S \tag{3}$$

where ϕ is porosity of material (m^3/m^3), ρ_w and ρ_s are density of water and solid (kg/m^3), respectively.

From Fourier's law, heat flux through porous material is computed by

$$q = -\lambda_{eff} \nabla T \tag{4}$$

where λ_{eff} is effective thermal conductivity (W/m K), and ∇T is temperature gradient in packed bed (°C/m).

Based on the experimental results of Aoki et al. [15], the effective thermal conductivity is further assumed to be a function of water saturation and is defined as

$$\lambda_{eff} = \frac{0.8}{1 + 3.7e^{-5.95S}} \tag{5}$$

Exchange of energy at surface of packed bed exposed to airflow can be calculated by

$$\lambda_{eff} \frac{\partial T}{\partial z} = -h_c (T_a - T_{sur}) + \dot{m}_w h_v \tag{6}$$

where h_c is convective heat transfer coefficient (W/m^2 K), $\dot{m}_w$ is mass flux of evaporation (kg/m^2 s) or rate of weight loss of water from porous media, h_v is latent heat of vaporization (J/kg), T_{sur} is temperature on material surface (°C), and T_a is air-flow temperature (°C).

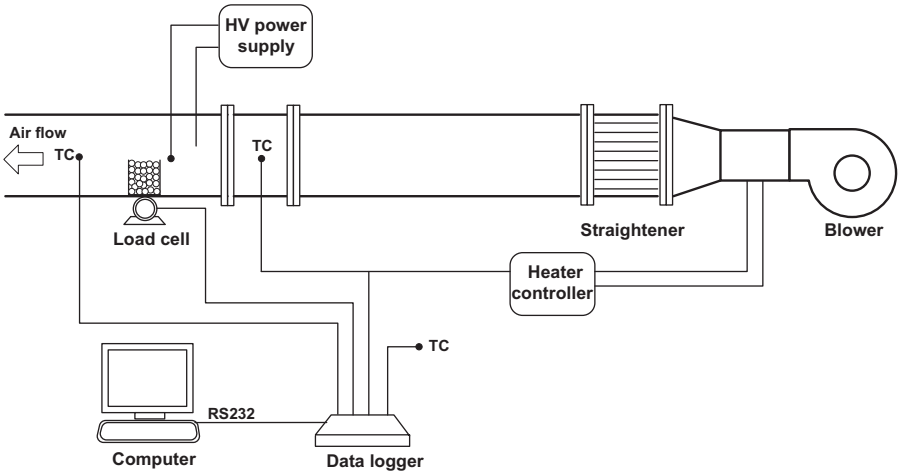

Fig. 2. Schematic diagram of experimental setup.

The relationship between the capillary pressure (p_c) and the water saturation is defined by using Leverett functions $J(S_{eff})$ [2,3], i.e.

$$p_c = p_g - p_l = \frac{\sigma}{\sqrt{K/\phi}} J(S_{eff}) \tag{7}$$

where S_{eff} is effective water saturation associated with the irreducible water saturation, K is permeability (m^2), and σ is surface tension (Pa m). Subscripts of g and l denote as gas and liquid phases, respectively.

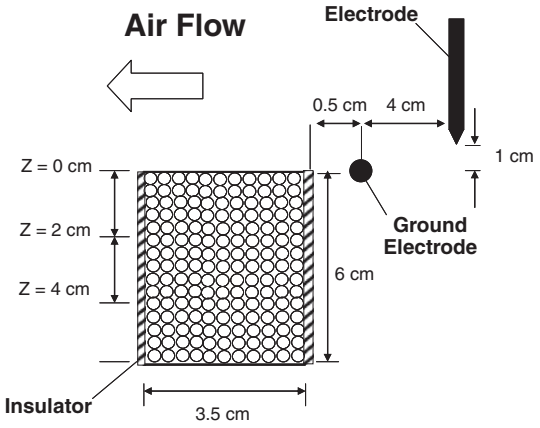

Fig. 3. Dimensions of packed bed and locations of electrodes.

3. Experimental setup and apparatus

Schematic diagram of experimental setup is shown in Fig. 2. The rig is an open system. Air is supplied from a blower and its temperature is increased by an electric heater. In order to control temperature of hot air, a thermocouple sensor (TC) is placed in front of the test section, where the cross-sectional area is $15 \times 15\ cm^2$. The high voltage power supply (LEYBOLD 521721) is used to create high-voltage electric fields.

As shown in Fig. 3, electrode wires are comprised of four copper positive discharge electrodes and a copper ground electrode. The discharge electrode wires are suspended from the top wall and are placed in the front of packed bed. Diameter of each discharge electrode is 0.025 mm and the space between each wire is 26 mm. Ground electrode is suspended horizontally across the test section, and its diameter is 0.25 mm.

Fig. 4 shows the configuration of the packed beds composed of glass bead, water and air. As shown in Fig. 4, the samples are prepared in the two configurations in the: a single-layered packed bed (uniform packed bed) with bed depth $\delta = 60$ mm ($d = 0.125$ (F bed) and $d = 0.38$ (C) bed), and a double-layered packed bed, respectively. The double-layered packed beds are arranged in different configurations in the: F–C bed (fine beads ($d = 0.125$, $\delta = 30$ mm) overlaying the coarse beads ($d = 0.38$ mm, $\delta = 30$ mm)), and C–F (coarse beads ($d = 0.38$ mm, $\delta = 30$ mm) overlaying the fine beads ($d = 0.125$, $\delta = 30$ mm)), respectively. The width and total length of all samples used in the experiments are 35 mm and 120 mm, respectively. The container of glass beads is made of acrylic plate with a thickness of 0.5 mm. Moreover, to control heat transfer from

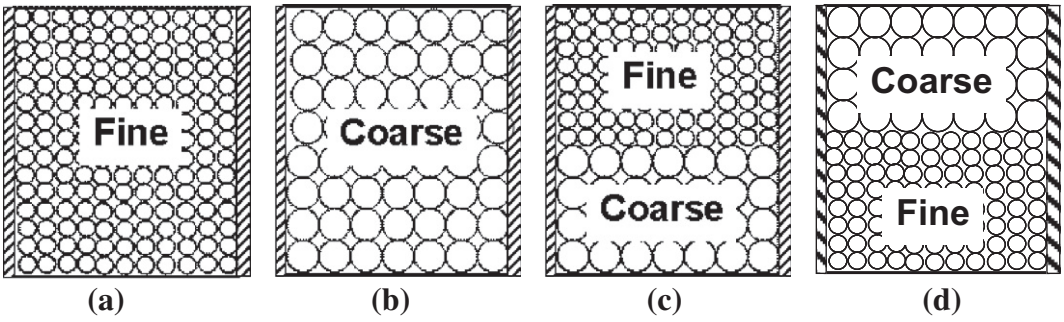

Fig. 4. Configuration of packed bed: (a) and (b) single layer, (c) F–C layer, and (d) C–F layer.

Table 1
Testing conditions.

Condition	Symbol	Value
Initial moisture	$X_{db,i}$	22–38%db
Drying temperature	T	50–60 °C
Ambient temperature	T_a	25 °C
Mean air velocity	U_b	0.33 m/s
Applied voltage	V	0, 10, 15 kV
Drying time	t	24–48 h
Glass beads	d	0.125, 0.38 mm

Table 2
Characteristics of water transport in porous media.

Diameter, d (mm)	Porosity, ϕ	Permeability, K (m^2)
0.125	~0.385	$\sim 8.41 \times 10^{-12}$
0.38	~0.371	$\sim 3.52 \times 10^{-11}$

hot air towards only the upper surface of packed bed, other sides are insulated by rubber sheet.

Temperature distribution within the sample are measured using fiber optic sensors (LUXTRON Fluroptic Thermometer, Model 790, Santa Clara, Canada, accurate to ±0.5 °C), which are placed in the middle plane of the sample at depth z = 0, 2, and 4 cm, which are measured away from the surface of the packed bed. In each test run, the weight loss of the sample is measured by a load cell.

In the experiments, the maximum electrical voltage is tested so that breakdown voltage will not occur. The details of testing conditions and characteristics of water transport in porous media are shown in Tables 1 and 2, respectively.

4. Results and discussion

In measuring the temperature in the packed bed, it is assumed that temperature is in state of thermodynamic equilibrium, thus temperatures of all phases, i.e. solid, liquid, and gas, are same. The average temperature of hot air measured at the front of test section is approximately 60 °C. Reynolds number ($R_e = U_b D_h/$) of airflow is 3049.

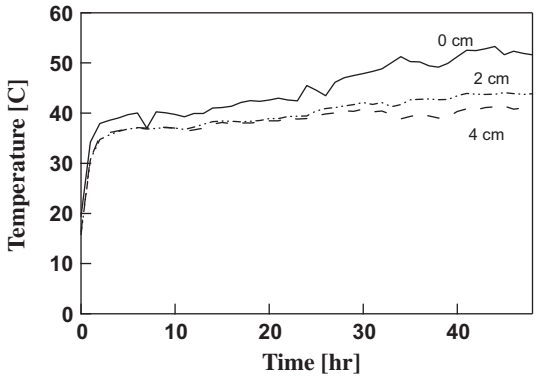

Fig. 6. Surface temperature (z = 0 cm) of packed bed with 0.125-mm bead in various voltages.

4.1. Effects of EHD on air flow

In order to observe the motion of airflow subjected to the electric fields, this study utilizes the incense smoke technique. A spotlight of 500 W is placed at the outlet of channel, and the light direction is opposite to the flow direction. Due to high speed of flow, the bulk mean velocity is reduced to 0.1 m/s. In addition, the motion of flow is continuously captured by a digital video camera recorder (SONY DCR-PC108/PC109E). As shown in Fig. 5, under the influence of EHD, airflow neighboring electrodes is induced by electric fields, and is circulated near the ground electrode. Moreover, it is observed that strength of vortex is proportional to the magnitude of electrical voltage applied.

4.2. Effects of heat and mass transfer on packed bed

Figs. 6 and 7 show the influence of EHD on temperature in packed bed with 0.125-mm bead at z = 0 and 4 cm, respectively. Clearly, when electric fields are applied, the temperature in packed bed increases faster. In addition, higher voltage applied gives rise to higher temperature. Moreover, EHD influences the surface temperature more than the inside. This is because EHD induces a sec-

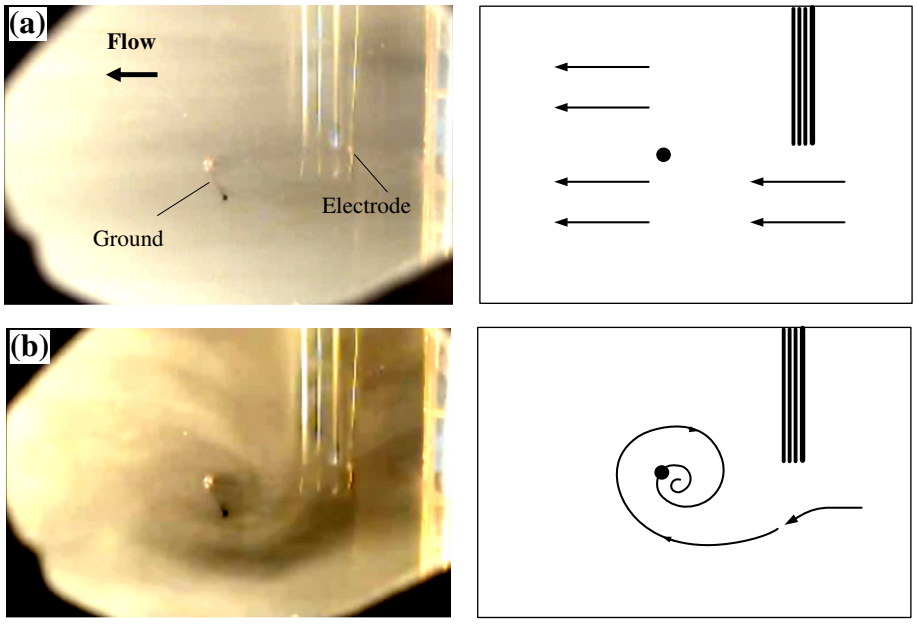

Fig. 5. Motion of air flow: (a) without electric fields, and (b) with electric fields at V = 10 kV.

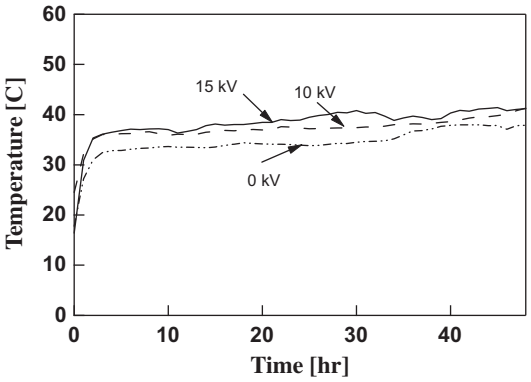

Fig. 7. Temperature of packed bed with 0.125-mm bead at $z = 4$ cm.

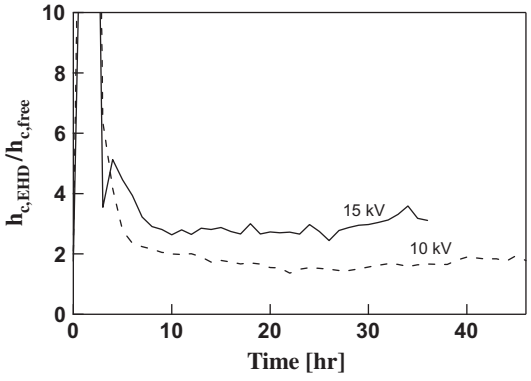

Fig. 8. Enhancement of heat transfer coefficient in case of packed bed with 0.125-mm bead.

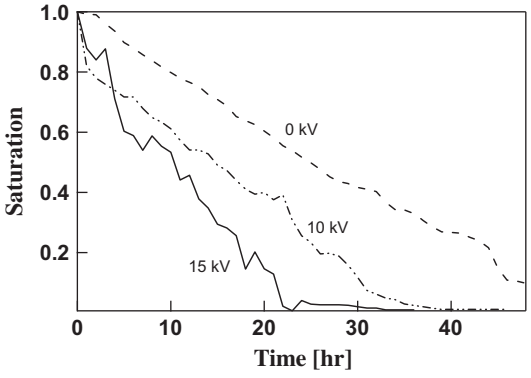

Fig. 9. Comparison on water saturation of packed bed with 0.125-mm bead in various voltages.

ondary flow, so-called Corona wind. The effect of this Corona wind circulating above packed bed enhances the mass transfer, and destabilizes the boundary layer on the surface. Consequently, convective heat transfer coefficient is enhanced, and then heat from hot-air flow can much transfers into packed bed. Therefore, the temperature of the cases with EHD is higher than that without EHD.

In this study, the augmentation of heat transfer due to EHD is defined as the ratio convective heat transfer coefficient with EHD to convective heat transfer coefficient with free air, i.e. $h_{c,EHD}/h_{c,free}$. As shown in Fig. 8, in warm-up period, this ratio increases rapidly. In addition, in constant drying period (constant surface temperature), the ratios are about 2 and 3 for cases with $V = 10$ and 15 kV, respectively.

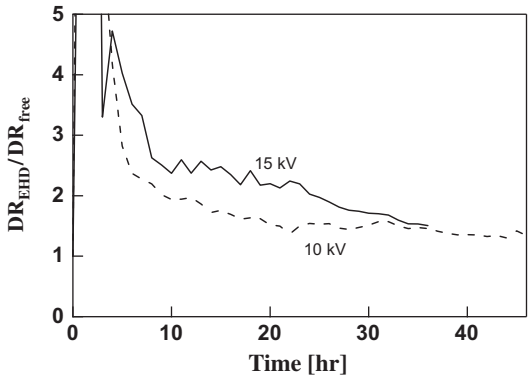

Fig. 10. Enhancement of rate of mass transfer in case of packed bed with 0.125-mm bead.

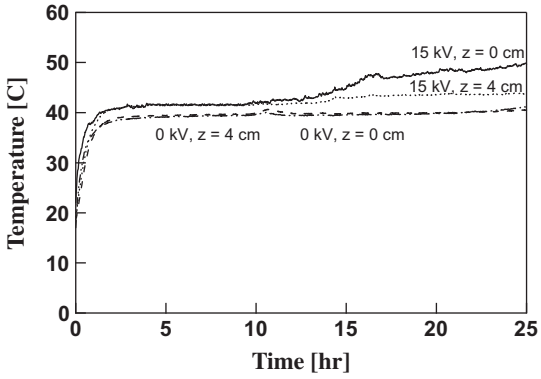

Fig. 11. Temperature of packed bead with 0.38-mm bead in various voltages at $z = 0$ and 4 cm.

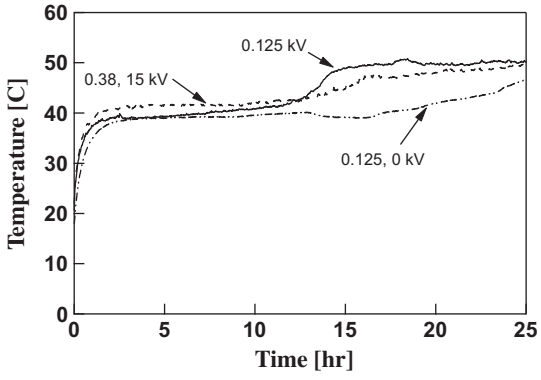

Fig. 12. Comparison on surface temperature ($z = 0$ cm) of packed bead with 0.38-mm and 0.125-mm beads.

As shown in Fig. 9, with voltage applied, water saturation in packed bed is much more reduced, due to enhancement of mass transfer. In constant rate of drying period, the drying rate with EHD approximately being 2–2.5 higher than that with hot-air flow only, as shown in Fig. 10.

Heat transfer in packed bed with big beads (0.38 mm) is shown in Fig. 11. Without EHD, difference of temperature between surface and inside is very small. Due to the influence of EHD, temperature difference is clearly observed. In addition, an increase in temperatures is much higher than that in the case without electric fields.

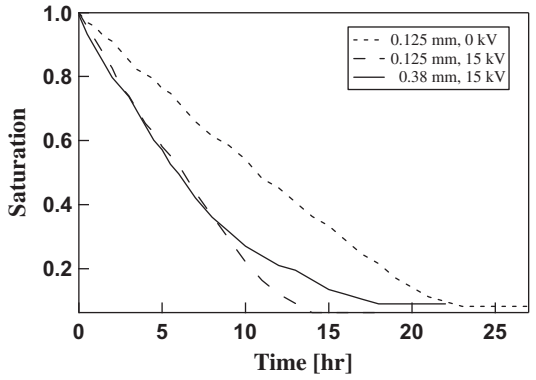

Fig. 13. Comparison on saturation in packed bead with different glass bead sizes.

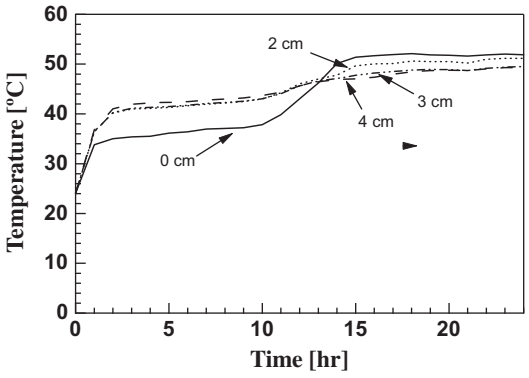

Fig. 15. Temperature in F–C packed bed when $V = 15$ kV.

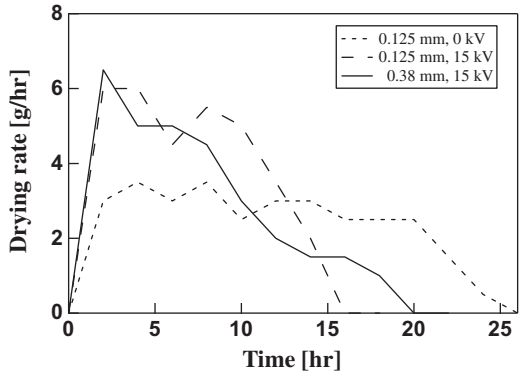

Fig. 14. Comparison on drying rate in packed bead with different glass bead sizes.

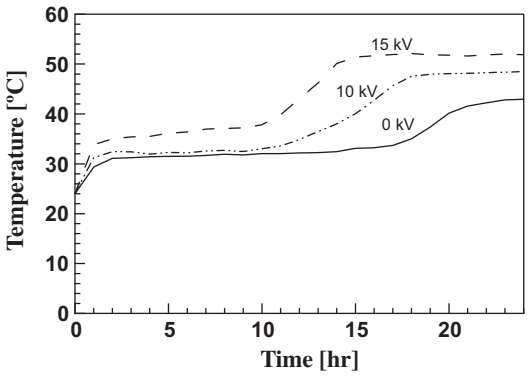

Fig. 16. Temperature at $z = 0$ cm in F–C packed bed in various voltages.

4.3. Effect of glass bead size

In the case of a single-layered packed bed, the moisture content continuously decreases towards the surface. The decrease in surface saturation leads to a saturation gradient, which draws liquid water towards the surface through capillary action while water vapor moves towards the surface due to a gradient in the vapor partial pressure.

The following results are concerned with the effect of particle size on moisture migration mechanism and heat transfer under the same conditions for the single-layered packed bed. As shown in Fig. 12, after a constant rate of drying period, surface temperature in packed bed with small bead (0.125 mm) rapidly increases, while the case in packed bed with big bead (0.38 mm), temperature gradually increases. As clearly seen in Fig. 13, saturation in small bead case decreases faster than that in big bead case. In addition, high rate of drying in small bead case remains longer than that in big bead case, as shown in Fig 14. This is because effect of capillary pressure in small bead case is higher than that in the big bead case. As shown in Table 2, porosity of packed bed with small bead is larger than that of packed bed with big bead. In addition, from Eq. (7), if $(\sigma J(S_{eff}))_{\text{fine}} \sim (\sigma J(S_{eff}))_{\text{coarse}}$ then $p_{c,\text{fine}} > p_{c,\text{coarse}}$. It means that in the case of same saturation, a smaller particle size corresponds to a higher capillary pressure. With higher capillary pressure, it can cause moisture to reach the surface at a higher rate. Therefore, more moisture is transferred from inside packed bed towards the surface.

In fact, in drying period, heat flux from hot-air flow transfers to water in packed bed for evaporation. If packed bed contains a high saturation level, then an increase of its temperature will be slow. This causes temperature in big bead case to be lower than that in small bead case.

4.4. Effects of layered arrangement

In case of double-layered packed bed, in order to measure the temperature on the interface layer, one more fiber optic wire is placed at $z = 3$ cm.

Temperature distributions in the case of double-layered packed bed (F–C bed and C–F bed) are quite different from the results in single-layered cases. Figs. 15 and 16 show temperature in packed bead of F–C case. As shown in Fig. 15, in the warm-up period, all temperatures in this packed bed rise up steadily. Later, they remain constant, and the surface temperature of packed bed is lowest. Until a certain time, the temperature on surface increases rapidly, and is higher than temperature in the other layers due to the effect of capillary pressure difference. From the above discussion, capillary pressure in small bead case is higher than that in big bead case. In the initial period, if both layers have the same amount of saturation, then there will be the difference of capillary pressure. Therefore, effect of capillary action in the fine bead layer (upper layer) will induce the moisture from the coarse bead layer (the lower layer) to the fine bead layer. This causes void in the lower layer to be filled with more of the vapor phase. Therefore, with a same heat flux, temperature in the lower layer becomes higher. As moisture evaporating process proceeds, temperatures of porous packed are constant, while heat is used for changing phase. Until a certain time, the surface becomes dry as heat will mainly transfer with conduction. Consequently, temperature in the upper layer rises up again when drying zone starts to appear, and the temperature of surface layer is higher than the other layers. Effect of voltage applied on heat transfer in F–C packed bed is shown in Fig. 16. With higher voltage, surface temperature of packed bed reaches a certain temperature faster.

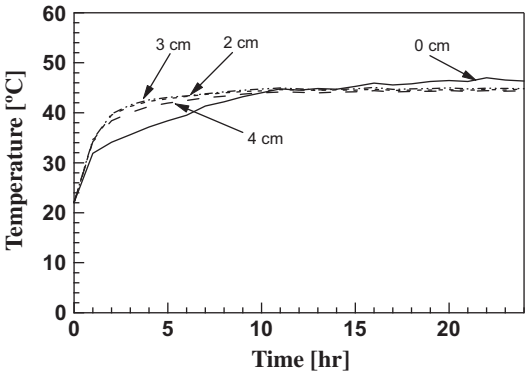

Fig. 17. Temperature in C–F packed bed when $V = 15$ kV.

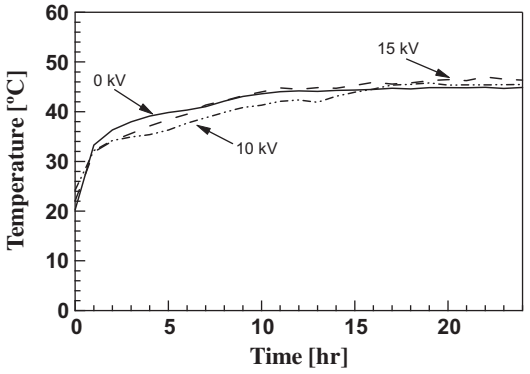

Fig. 18. Temperature at $z = 0$ cm in C–F packed bed in various voltages.

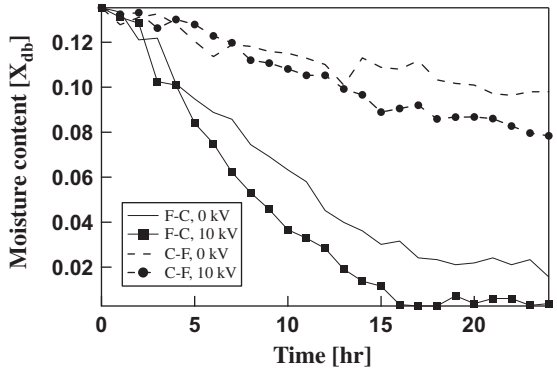

Fig. 19. Comparison on moisture content in double-layered packed bed in various cases.

Figs. 17 and 18 show the results when coarse beads overlay fine beads. Unlike F–C case, without and with electric fields, the temperature in each depth is not much different. In addition, the surface temperature is highest. This is because moisture in the coarse layer (the upper layer) slowly transfers to the surface, and this effect retards the moisture transfer from the lower layer towards the upper.

It is evidenced in Fig. 19 that when the drying process reaches a certain time, moisture content in F–C packed bed is in low level, while the moisture content in C–F packed bed is still high. In other words, the moisture removed from C–F cases is much lower than that from F–C cases. As mentioned above, effect of capillary pressure difference suppresses a certain amount of moisture in C–F cases to transfer toward the surface. With influence of EHD, the drying rate is increased. In addition, rate of drying of F–C cases is about 3.13–3.67 times higher than that of C–F case. Moreover, with voltage applied, the drying rate is improved about 1.5–1.97 times.

5. Conclusions

Effect of electrical voltage, particle sizes, and layered arrangement on heat and mass transfer in the porous packed beds are experimentally investigated and analyzed in this paper. The following paragraph summarizes the conclusions of this study:

1. Effects of Corona wind circulating above packed bed enhance the convective heat transfer coefficient and evaporation rate on the packed-bed surface exposed to hot-air flow, resulting in enhancement of heat and mass transfer in the packed bed. In addition, the degree of enhancement of heat and mass transfer is dependent on the magnitude of voltage applied.
2. The effects of particle size are clarified. The drying rate in the small bead case is higher than that in the big bead case. This is because of the higher capillary pressure for the packed bed with small bead: moisture in packed bed can be substantially removed towards the material surface.
3. Due to the effect of capillary pressure difference, heat and mass transfer in double-layered case and the single-layered case behave differently. With retarding effect on moisture motion to the upper layer of the C–F case, relatively small amount of moisture moves to the upper layer, resulting in a low temperature. In F–C cases, effect of capillary pressure difference enhances moisture in the lower layers to move towards the upper layers. With voltage applied, the drying rate is improved about 1.5–1.97 times. In addition, the drying rate of F–C cases is about 3.13–3.67 higher than that of C–F cases.

Acknowledgement

The authors are pleased to acknowledge Thailand Research Fund (TRF) for supporting this research work.

References

[1] F. Gori, G. Gentili, L. Matini, Microwave heating of porous media, ASME J. Heat Transfer 109 (1987) 522–525.
[2] A.E. Drouzasam, H. Dchubert, Microwave application in vacuum drying of fruits, J. Food Eng. 28 (1996) 203–209.
[3] J. Yongsawatdigul, S. Gunasekaran, Microwave–vacuum drying of cranberries: part I. Energy use and efficiency, J. Food Process. Preserv. 20 (1996) 121–143.
[4] P. Ratanadecho, K. Aoki, M. Akahori, Experimental and numerical study of microwave drying in unsaturated porous material, Int. Commun. Heat Mass Transfer 28 (5) (2001) 605–616.
[5] P. Ratanadecho, K. Aoki, M. Akahori, Influence of irradiation time, particle sizes, and initial moisture content during microwave drying of multi-layered capillary porous materials, J. Heat Transfer 124 (2002) 151–161.
[6] W. Cha-um, P. Rattanadecho, W. Pakdee, Experimental analysis of microwave heating of dielectric materials using a rectangular wave guide (MODE: TE10) (Case study: water layer and saturated porous medium), Exp. Therm. Fluid Sci. 33 (2009) 472–481.
[7] C. Sandua, Infrared radiative drying in food engineering: a process analysis, Biotechnol. Prog. 2 (3) (1986) 109–119.
[8] N. Sakai, T. Hanzawa, Application and advances in infrared heating in Japan, Trends Food Sci. Technol. 5 (11) (1994) 357–362.
[9] D. Nowak, P.P. Lewicki, Infrared drying of apple slices, Innov. Food Sci. Emerg. Technol. 5 (2004) 353–360.
[10] J. Wang, K.C. Sheng, Modeling of multi-layer far-infrared dryer, Drying Technol. 22 (2004) 809–820.
[11] A. Alem-Rajabif, F.C. Lai, EHD-enhancement drying of partially wetted glass beads, Drying Technol. 23 (1995) 597–609.
[12] F.C. Lai, K.W. Lai, EHD-Enhanced drying with wire electrode, Drying Technol. 20 (7) (2002) 1393–1405.
[13] T.I.J. Goodenough, P.W. Goodenough, S.M. Goodenough, The efficiency of corona wind drying and its applicaition to the food industry, J. Food Eng. 80 (2007) 1233–1238.

[14] E. Schröder, A. Class, L. Krebs, Measurements of heat transfer between particles and gas in packed bed at low to medium Reynolds numbers, Exp. Therm. Fluid Sci. 30 (2006) 545–558.

[15] K. Aoki, M. Hattori, M. Kitamura, N. Shiraishi, Characteristics of heat transport in porous media with water infiltration, ASME/JSME Therm. Eng. Proc. 4 (1991) 303–308.